Sensor Review

Using no-parameter statistic features for texture image retrieval

Xianqiang Zhu, Zhenfeng Shao,

Article information:

To cite this document:
Xianqiang Zhu, Zhenfeng Shao, (2011) "Using no-parameter statistic features for texture image retrieval", Sensor Review, Vol. 31 Issue: 2, pp.144-153, https://doi.org/10.1108/02602281111110004
Permanent link to this document:
https://doi.org/10.1108/02602281111110004

Downloaded on: 15 January 2019, At: 02:47 (PT)
References: this document contains references to 24 other documents.
To copy this document: permissions@emeraldinsight.com
The fulltext of this document has been downloaded 847 times since 2011*

Users who downloaded this article also downloaded:

(1997),"Asymptotic approximations for the distributions of the (h-, φ-)-divergence goodness-of-fit statistics: application to Renyi's statistic", Kybernetes, Vol. 26 Iss 4 pp. 442-452 https://doi.org/10.1108/03684929710176449

(1970),"PLANS FOR A NEW SYSTEM OF BUSINESS STATISTICS", Aslib Proceedings, Vol. 22 Iss 7 pp. 309-319 https://doi.org/10.1108/eb050247

Access to this document was granted through an Emerald subscription provided by emerald-srm:155010 []

For Authors

If you would like to write for this, or any other Emerald publication, then please use our Emerald for Authors service information about how to choose which publication to write for and submission guidelines are available for all. Please visit www.emeraldinsight.com/authors for more information.

About Emerald www.emeraldinsight.com

Emerald is a global publisher linking research and practice to the benefit of society. The company manages a portfolio of more than 290 journals and over 2,350 books and book series volumes, as well as providing an extensive range of online products and additional customer resources and services.

Emerald is both COUNTER 4 and TRANSFER compliant. The organization is a partner of the Committee on Publication Ethics (COPE) and also works with Portico and the LOCKSS initiative for digital archive preservation.

*Related content and download information correct at time of download.

Downloaded by Wuhan University At 02:47 15 January 2019 (PT)

Downloaded by Wuhan University At 02:47 15 January 2019 (PT)

Research article

Using no-parameter statistic features for texture image retrieval

Xianqiang Zhu and Zhenfeng Shao
State key Laboratory for Information Engineering in Surveying, Mapping and Remote Sensing,
Wuhan University, Wuhan, China

Abstract

Purpose – The purpose of this paper is to analyze the spectrum influence between radon transform and log-polar transform when rotation and scale effect is eliminated. The average retrieval performance of wavelet and NSCT with different retrieval parameters is also studied.

Design/methodology/approach – The authors designed a multi-scale and multi-orientation texture transform spectrum, as well as rotation-invariant feature vector and its measurement criteria. Then a new two-level coarse-to-fine rotation and scale-invariant texture retrieval algorithm based on no-parameter statistic features was proposed. Experiments on VisTex texture database show that the algorithm proposed in this paper is appropriate for main orientation capturing and detail information description.

Findings – According to the experiments results, it was found that the combination of this two-level progressive retrieval strategy and multi-scale analysis method can effectively improve retrieval efficiency compared with traditional algorithms and ensure a high precision as well.

Originality/value – The paper presents a novel algorithm for rotation and scale-invariant texture retrieval.

Keywords Programming and algorithm theory, Image processing, Sensors

Paper type Research paper

Introduction

Texture is an importance feature for the field of image segmentation, image classification, and image retrieval. Early studies for texture analysis focused on the analysis of the first- or second-order statistics of textures, and stochastic models such as generalized Gaussian distribution, Markov random fields and autoregression (Van de Wouwer *et al.*, 1999, Liu *et al.*, 2007; Randen and Husoy, 1999; Smeulders *et al.*, 2000; Pietikäinen *et al.*, 2000). Recent developments in the spatial/frequency analysis such as Gabor filters (Arivazhagan *et al.*, 2006; Zhang *et al.*, 2000; Haley and Manjunath, 1999), wavelet transforms (Cheng *et al.*, 2005; Li *et al.*, 2005), steerable pyramid decomposition (Montoya-Zegarra *et al.*, 2007) and polar or radon transform (Chen and Chen, 2008; Lo *et al.*, 2004; Portilla and Simoncelli, 2000) provide good multi-resolution analytical tools for texture analysis and classification. Experimental results show that these approaches can achieve a high accuracy rate. However, when we get texture images the different sensors' angle and resolution cause texture rotation and scale change, how to identify the same textures following human vision principle from rotation texture database is an essential issue in texture image analysis (Zeng *et al.*, 2005).

In the context of rotation-invariant image retrieval, constructing a representative rotation-invariant texture feature vector and the corresponding measurement methods is the crucial property in a number of applications. At the current state of rotation-invariant image retrieval, multi-scale analysis and rotation-reducing transform algorithm are proved as effective solution by many researchers. Such as Montoya's retrieval uses dominant energy direction as rotation-invariant and scale-invariant image descriptor based on steerable pyramid decomposition (Montoya-Zegarra *et al.*, 2008), Chi-Man (Chi-Man, 2003) and Kourosh's (Jafari-Khouzani and Soltanian-Zadeh, 2005) experiments employ the combination of wavelet and log-polar or radon transform as rotation-invariant feature extraction method for texture retrieval, Franci, etc. study on the use of standardizing energy vector which is based on Gabor and Gaussian coefficience for rotation texture identification (Franci and Stanislav, 2003). These above experiments are usually got a better result but there are several obvious drawbacks. For example, Gabor filter and wavelet coefficients is not the most sparse representation of image and it cannot take full use of the original data's geometrical features and edge distribution information, on the other hand when we use different measurement method, the recognition capability of log-polar and radon transform need further analysis.

In this paper, a series of multi-scale multi-orientations texture spectrum and a rotation-invariant feature vector are

The current issue and full text archive of this journal is available at
www.emeraldinsight.com/0260-2288.htm

Sensor Review
31/2 (2011) 144–153
© Emerald Group Publishing Limited [ISSN 0260-2288]
[DOI 10.1108/02602281111110004]

This article is supported by National 973 Basic Research and Development Program project (No. 2010CB731800); National High Technology Research and Development Program of China (863 Program) (No. 2009AA121404); National Natural Science Foundation program (No. 40801165, No. 10978003); Outstanding Doctoral Dissertation Nurture Fund of Wuhan University; Self-research program for Doctoral Candidates (including Mphil-PhD) of Wuhan University in 2008.

designed, and then a new gradual multi-scale rotation-invariant texture retrieval process is provided. In the algorithm, after rotation reduction NSCT is used to get multi-scale and multi-orientation spectrum, then its low- and high-frequency bands are employed for texture images' coarse retrieval and fine retrieval. The experiments on (http://vismod.media.mit.edu/vismod/imagery/VisionTexture/vistex.html) VisTex texture database shows that log-polar transform is good at preserving scale and direction detail, and NSCT get more representation feature than wavelet. Compare to traditional methods, this multi-scale texture spectrum and progressive retrieval strategy could effectively improve the efficiency of texture image retrieval.

Related theory about rotation-invariant texture retrieval

Log-polar transformation to reduce rotation effects

The log-polar transform algorithm is divided into two major steps. Taking a N*N image for example, In the first step, the radius of the inscribed circle of the given square image is used as a scan line to sample S times from 0° to 360° to produce its equivalent $S^{*}\lfloor N/2 \rfloor$ polar form (as shown in Figure 3(a). So, formally, a polar form can be computed as formula (1):

$$p(a,r) = f\left(\left\lfloor \frac{N}{2} \right\rfloor + \left\lfloor r\cos\left(\frac{2\pi a}{S}\right)\right\rfloor, \left\lfloor \frac{N}{2} \right\rfloor - \left\lfloor r\sin\left(\frac{2\pi a}{S}\right)\right\rfloor \right) \quad (1)$$

And then, logarithm functions are applied to all radii values in the polar form and their outputs are then quantized into R bins. Hence, a $S \times R$ log-polar image for the given $N \times N$ image is produced (as shown in Figure 3(b)). The logarithm functions can be formally defined as formula (2):

$$lp(i,j) = p\left(i, \left\lfloor \frac{\log_2(j+2)}{\log_2(S+2)} \right\rfloor \cdot \left\lfloor \frac{N}{2} \right\rfloor \right) \quad (2)$$

Log-polar transform is used to eliminate or reduce the rotation of the input image, the rotation of angles are expressed as row shifted in the log-polar spectrum (as shown in Figure 1(b). As shown in Figure 2, the log-polar images of texture images with different rotation angles and scales seem having only row shifts when compared with the log-polar image of the original texture. To generate the corresponding log-polar image, the given image and the polar image are both scanned once. So the log-polar transform is also quite efficient with only $O_{(n)}$ computational complexity, where n is the number pixels in the given image.

Figure 1 Log-polar transform

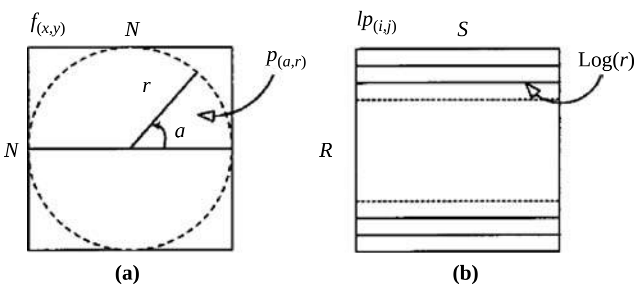

Notes: (a) Polar transform; (b) applying quantization on the logarithm of all radii to produce the log-polar image

Figure 2 Sample Texture (1.2.02) from VisTex album with different rotation angles (α in degrees) and scales (s) and their corresponding log-polar images

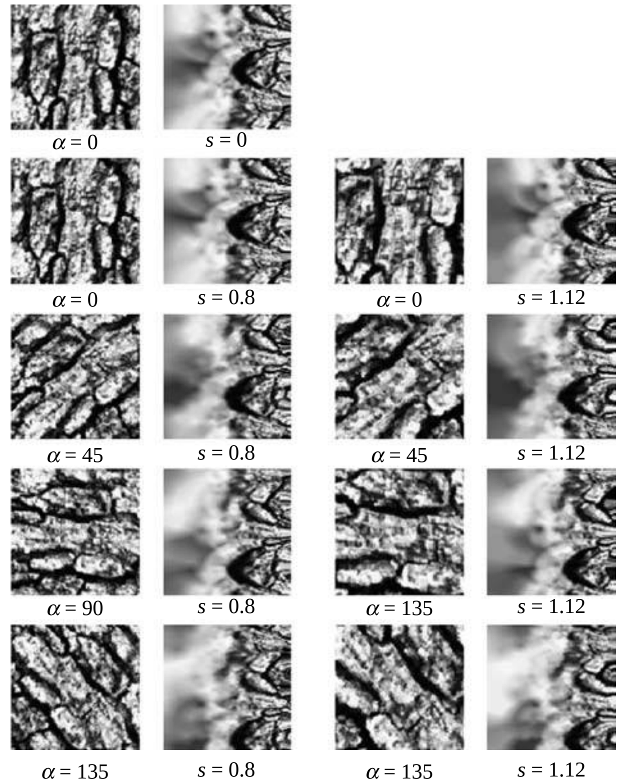

Note: Images in the first row are original image and its corresponding log-polar image

Multi-scale texture analysis method

NSCT is an improved transform based on contourlet transform proposed by M.N. Do, etc. (Lin and Zhang, 2008). It inherits the multi-scale and multi-orientation advantages of contourlet transform, also obtains the image geometry structure, and extracts the image edges into different scales and frequency sub-bands. Owing to the elimination of subsample, contourlet transform has translate-invariant as well as eliminating the Gibbs phenomenon. The representative of the contourlet sub-band coefficients for the texture image is better than the wavelet transform which can only decompose in limited directions, it is appropriate for texture directional analysis.

NSCT is shown as Figure. 3. Through this filter bank, the image is divided into low-frequency sub-band and high-frequency sub-band, and iterative filter for the low-frequency is done to implement multi-structure. NSCT employs non-subsampled pyramid filter and non-subsampled directional filter, the sub-band image is the same size as the original image, the redundancy reaches as $1 + \sum_{j=1}^{\mathcal{J}} 2^{l_j}$, where $\mathcal{J}$ is the decomposition level. As the increase of the redundancy, NSCT owns shift invariant. Figure 4 shows the example of NSCT with three scales each scale owns 4, 8, 16 direction bands, which shows as b-d.

Downloaded by Wuhan University At 02:47 15 January 2019 (PT)

Figure 3 NSCT transform

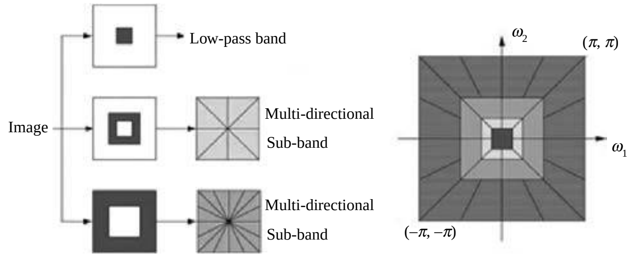

Notes: (a) Non-subsample filter bank that implements NSCT; (b) idealized frequency partitioning obtained with the proposed structure

Rotation and scale-invariant texture image retrieval

Construction of rotation and scale-invariant feature vector

The first step of rotation-invariant texture retrieval algorithm is radon or log-polar transform which is used to convert the texture image's disclination to row-shift or column-shift. Then in order to extract the multi-scale and multi-direction feature vector by multi-scale analysis method which is charactered with rotation and scale invariant. Here, we take radon transform and NSCT transform as example which is shown as Figure 5.

In Figure 5, after log-polar transform the texture image is decomposed into 28 spectrums with the direction of the three scales of 16, 8 and 4. From the diagram, we can see that the image detail information is decomposed into several sub-directions in 3 scales. But in different orientation band, the energy values are different according to the difference of the texture distribution. The energy is represented by Shannon entropy, which can be computed as formula (3):

$$E(x) = -\sum_{i=1}^{n} \tilde{x}_i \ln \tilde{x}_i \tag{3}$$

where $\tilde{x}$ is the standardized histogram, and $\tilde{x}_i \in (0, 1)$. According to formula (3), the energy of NSCT coefficients in different orientations and scales are shown in Table I.

Figure 4 NSCT example

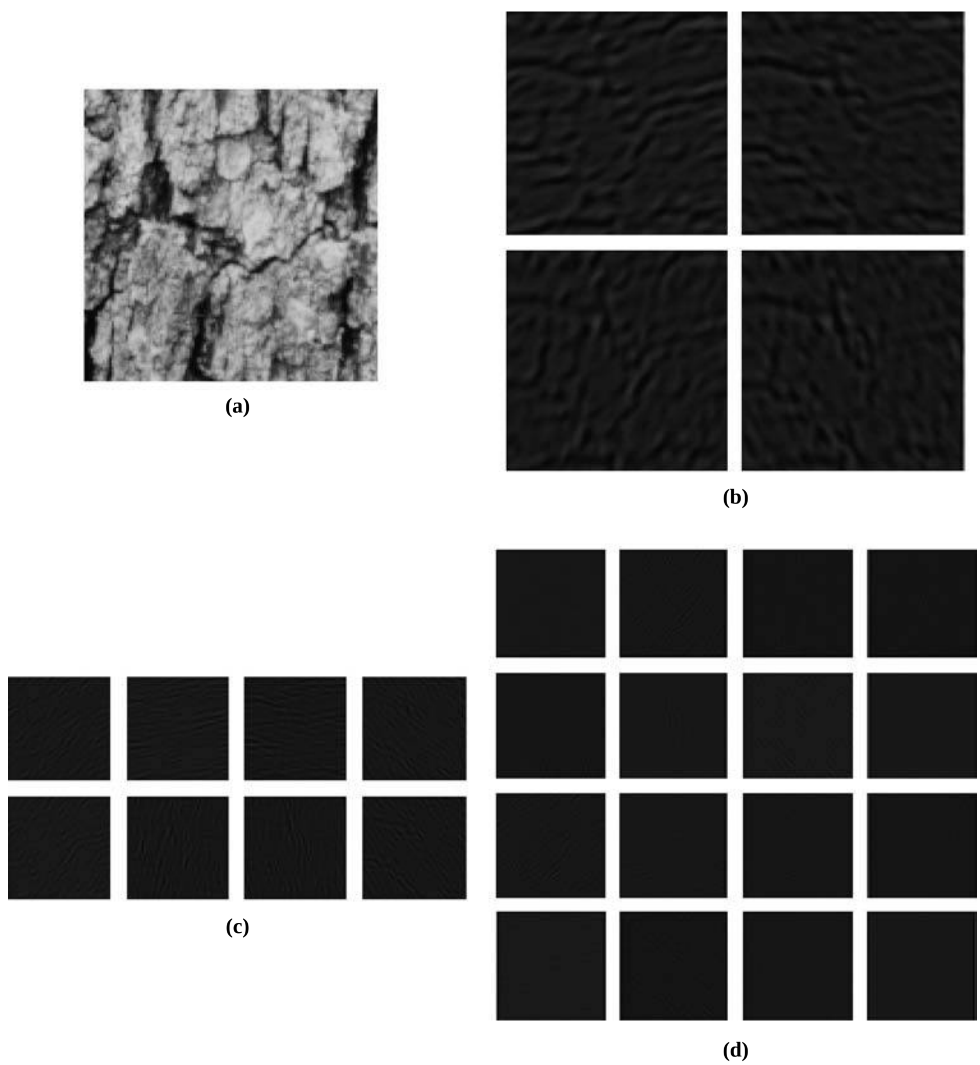

Notes: (a) Original image; (b) the first scale bands; (c) the second scale bands; (d) the third scale bands

Downloaded by Wuhan University At 02:47 15 January 2019 (PT)

Downloaded by Wuhan University At 02:47 15 January 2019 (PT)

Figure 5 Log-polar and NSCT transform spectrum of texture image

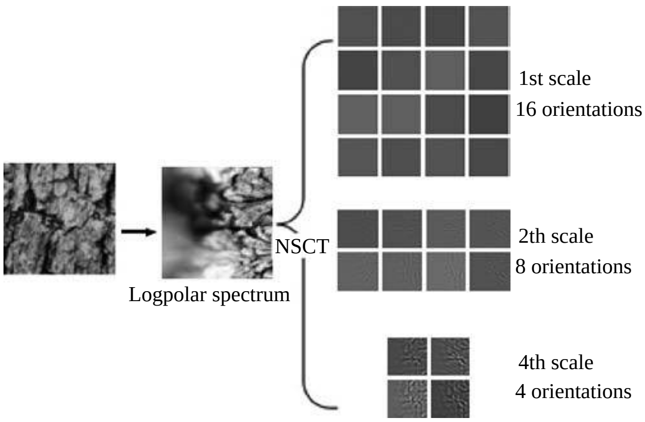

Table I Energy distribution of NSCT directional bands

	Scale		
Direction	**1**	**2**	**3**
Direction 1	0.861	1.114	1.517
Direction 2	0.757	0.977	1.521
Direction 3	0.813	0.977	1.585
Direction 4	0.743	1.113	1.582
Direction 5	0.743	1.188	–
Direction 6	0.812	1.238	–
Direction 7	0.738	1.211	–
Direction 8	0.849	1.182	–
Direction 9	0.991	–	–
Direction 10	0.857	–	–
Direction 11	1.007	–	–
Direction 12	0.946	–	–
Direction 13	0.900	–	–
Direction 14	0.932	–	–
Direction 15	0.828	–	–
Direction 16	0.968	–	–

From Table I, this energy difference has an important effect on the visual of the texture's roughness extent. Usually, human eyes are more sensitive to the sub-band with larger energy value. In Chapter 3.2, energy feature of each sub-band is taken as a distance weight to measure the differences between the values of texture and enhance the ability of distinguishing the features of texture in the algorithm.

The spectral histogram and the associated distance measure provide a unify similarity measure for images. Because the marginal distribution is independent of image sizes, any two image patches can be compared using the spectral histogram. So the spectral histogram is a simple and effective statistical property which is adaptive for rotation displacement measurement. So we combined it with NSCT directional spectrums (Liu and Wang, 2003), a new texture feature descriptor spectrum histogram is extracted. From Figure 6, different sub-bands own similar histogram distribution, high peak around zero value, but long tails at both sides. And its low band preserves abundant contour information, so the low band histogram can be used as coarse judgment criterion.

From the graph named c, we can see that the peak value of the 12 bands are various from each other, which means that the distributed energy among NSCT coefficients are not same from each other. Usually, information is integrated in several bands, if we increase those bands feature weight, a more representative feature vector will be got. This is also the foundation for the design of energy sensitive measure criterion in following section.

Energy-sensitive similarity measurement

From Figure 4, we can see orientation sub-bands owns same distribution. It is assumed that high-frequency sub-bands are independent and subject to the probability density function $p(X;\theta_i)$. The distance between the two texture images can be calculated by Kullback-Leibler divergence (Shao *et al.*, 2010) as follows:

$$D(p(X;\theta_i)\|p(X;\theta_j)) = \int p(X;\theta_i)\log\frac{p(X;\theta_i)}{p(X;\theta_j)}\,dx \qquad (4)$$

Discrete KL divergence of the spectrum histogram shows as formula (5):

$$KL(H_{I1}, H_{I2}) = \sum_{\alpha=1}^{K}\sum_{z}\left(H_{I1(z)}^{(\alpha)} - H_{I2(z)}^{(\alpha)}\right)\log\frac{H_{I1(z)}^{(\alpha)}}{H_{I2(z)}^{(\alpha)}} \qquad (5)$$

where K is orientation number, formula (5) is derived on the condition that the orientation sub-bands are independent. Actually, the NSCT transform coefficients have relevance. And according to the energy statistics of orientation sub-bands in 2.2 and the feature of human visual perception discriminates the texture, It can be seen that the relative texture energy in different directions have an important impact on the visual effects on the roughness of the texture. So, weighting the feature in the corresponding direction by the percentage of energy can emphasize the sensitive feature of the human visual perception. The KL weighted distance formula is calculated as equation (6):

$$KL(H_{I1},\ H_{I2}) = \sum_{\alpha=1}^{K} w(\alpha)\sum_{z}\left(H_{I1(z)}^{(\alpha)} - H_{I2(z)}^{(\alpha)}\right)\log\frac{H_{I1(z)}^{(\alpha)}}{H_{I2(z)}^{(\alpha)}} \qquad (6)$$

The weight value of the orientation sub-bands is $w(\alpha) = E_\alpha/\sum_i E_i$, $E = \sum_i \log x_i^2$ is the energy. As formula (7) contains logarithm operation, it has low computational efficiency. Therefore, the first-order approximation distance χ^2 is selected to reduce the complexity effectively, the formula is:

$$\chi^2(H_{I1},\ H_{I2}) = \sum_{\alpha=1}^{K} w(\alpha)\sum_{z}\frac{\left(H_{I1}^{(\alpha)}(z) - H_{I2}^{(\alpha)}(z)\right)^2}{H_{I1}^{(\alpha)}(z) + H_{I2}^{(\alpha)}(z)}$$
$$= \sum_{\alpha=1}^{K} w(\alpha)\chi^2\left(H_{I1}^{(\alpha)}, H_{I2}^{(\alpha)}\right) \qquad (7)$$

The algorithm of rotation and scale-invariant texture retrieval

(1) Extraction of rotation and scale-invariant vector

After applying row-shift invariant NSCT transform to the row shifted log-polar image, the NSCT coefficients thus generated are rotation and nearly scale invariant. So the histogram of NSCT directional spectrums can be acted as rotation and scale invariant vector.

Downloaded by Wuhan University At 02:47 15 January 2019 (PT)

Figure 6 Radon and NSCT transform spectrum of texture image

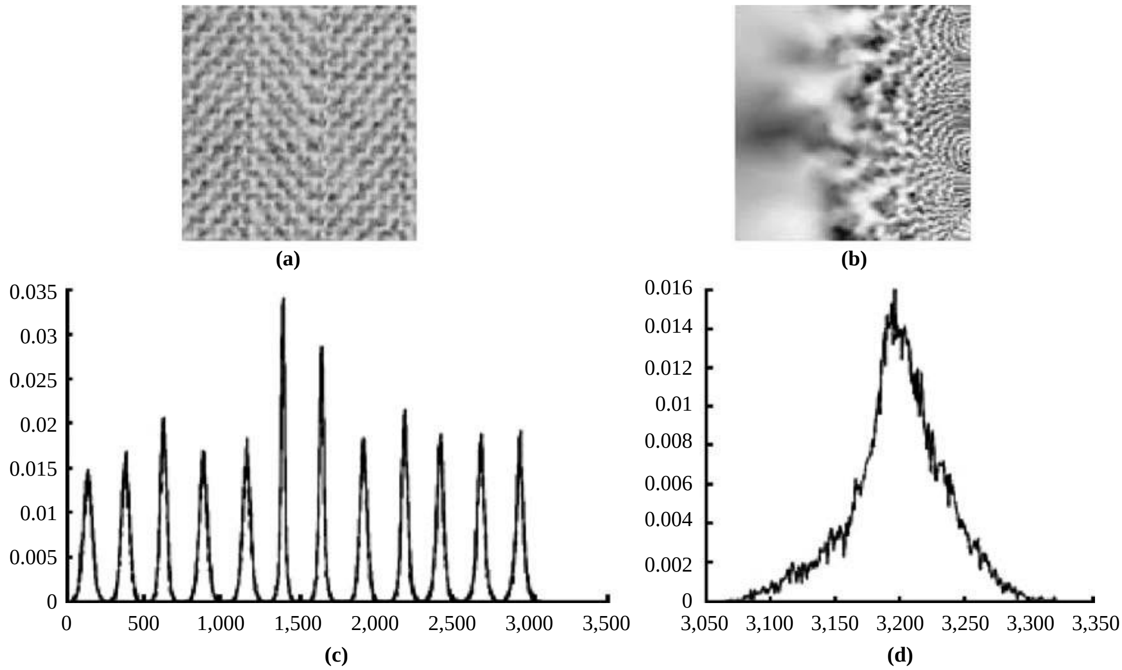

Notes: (a) Displays original texture; (b) radon spectrum; (c) 12 directional spectrum histograms after NSCT; (d) low-band spectrum histogram

First, for an $M \times N$ image, apply log-polar transform to produce a $S \times R$ log-polar image, here we set $S = M$, $R = N$.

Second, row-shift invariant transform NSCT is used to decompose log-polar image, producing k scale levels and each scale owns 2^{l_k} direction sub-bands, where l_k belongs to positive integer dataset.

During the third step, calculate energy and spectrum histogram vectors:

$$W = \{w_i, i = 1, 2, \ldots, n\} \quad H = \{H_i, i = 1, 2, \ldots, n\}$$

Step 4, output the feature vector $f = \{W, H\}$ as the rotation and scale invariant signature for the given image.

The details of the algorithm are shown as Figure 7.

(2) The flow chart of rotation and scale-invariant texture retrieval
In order to improve retrieval efficiency, we employ a two-step progressive retrieval strategy which is from coarse to fine. First, the low-frequency sub-band histogram of NSCT transform is used for filtering the image with great differences and narrowing the target range, second, high-frequency sub-band histogram of NSCT transform is used for measuring the similarity of the detailed information in texture image, acting as fine texture image retrieval. Finally, In accordance with the size of the similarity of the results, K images will be returned. The multi-scale and multi-orientation progressive retrieval algorithm is beneficial to comprehensively consider the local and whole texture features of texture image and can effectively improve retrieval efficiency. As shown in Figure 7, the target texture feature database is generated off-line. In the dashed border box, there are the generation steps of the rotation-invariant feature vector which extract from query image and texture feature database.

Figure 7 Extraction of rotation and scale-invariant vector

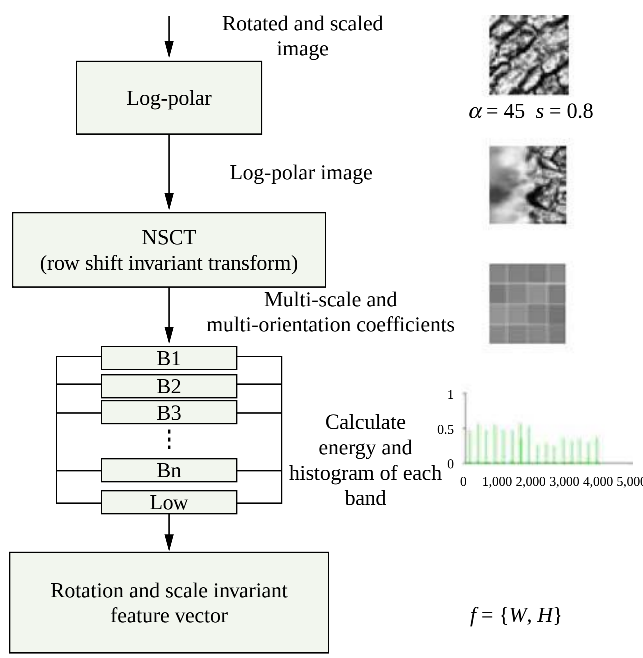

Experiments and analysis

The effectiveness of the proposed log-polar NSCT signatures for rotation and scale-invariant texture retrieval has been well tested via several experiments using a set of 30 natural texture images, each image contains 512×512 pixels, as shown in Figure 8, from the VisTex's texture album (Manjunath and Ma, 1996).

Figure 8 The flow chart of rotation and scale-invariant texture retrieval

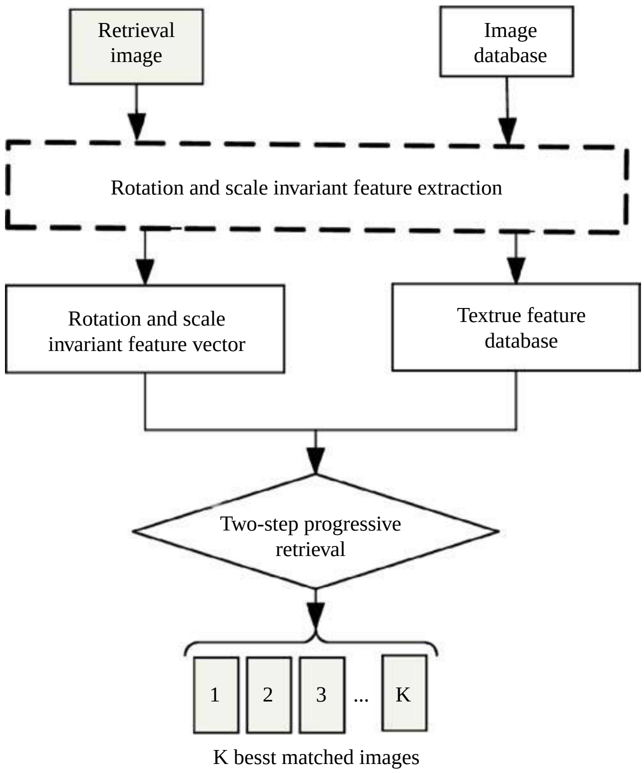

Note: Where the details of rotation and scale-invariant feature extraction step is shown as Figure 8

Three series of experiments were conducted to demonstrate the discriminating power of our system for recognizing texture patterns. In the first series of experiments, we evaluated the effectiveness of the proposed rotation and scale-invariant feature representation on texture images with rotation or scale changes only. The second series of experiments are used to evaluate the distance measure criterions in our retrieval stage. The last series of experiments aimed at evaluating the effectiveness of our algorithm against other approaches: the radon transform and wavelet decomposition (Do and Vetterli, 2002; Manjunath and Ma, 1996).

According to our above three purpose, from the no rotated and no scaled version of the selected 30 textures, three different image datasets were generated: rotated-set, scaled-set and joint rotation and scale set.

For rotated-set, we extract 16 subsamples from original 512×512 images with different orientations (from 0 to 180° with 11° intervals), and then setting the new images' center as the origin, clips sub-image of 128×128 pixels to build the target texture image database. In this way, a dataset of 480 (30×16) texture images was created.

For scaled-set, we extract 16 subsamples from original 512×512 images with different scales (from 0.8 to 1.2 with 0.025 interval), and then setting the new images' center as the origin, clips sub-image of 128×128 pixels to build the target texture image database. In this way, a dataset of 480 (30×16) texture images was created.

For joint rotation and scale set, from each 512×512 texture image we extract 80 subsamples with different orientations (from 0 to 180° with 11° interval, the scale parameter ranges from 0.8 to 1.2 with 0.1 interval), and then setting the new images' center as the origin, clips sub-image of 128×128 pixels to build the target texture image database. Finally, a dataset of 2,400 (30×80) texture images was created.

Among the above three dataset, we assume the different orientations or scales images as the similar images to its original image class, which are shown as the b and c graph in Figure 9.

Experiments for images with rotation or scale changes only

In these experiments, rotated-set and scaled-set are employed to test the algorithm's sensitive to rotation or scale changes. The retrieval effectiveness was measured in terms of relevant retrieval average rate, i.e. the percentage of relevant images among the top N retrieved images.

Retrieval results are shown as Figures 10 and 11. The Figure 9 shows the average retrieval rates on separately six sub-databases such as 5, 10, 15, 20, 25, 30 classes rotated-set textures. The Figure 10 shows similar results on scaled-set. These two experiments both employ log-polar and NSCT to get multi-scale and multi-direction coefficients. NSCT employs Maxflat pyramidal decomposition and dmaxflat7 direction filter bank, the direction parameters are (Liu *et al.*, 2007; Randen and Husoy, 1999), the distance measure formula using χ^2-distance.

The rotation-invariant feature depends on the first part polar transform, the subsequent logarithm operation on the polar-transformed image reduces the effects of size or scale variations of similar images on the resulting image feature. As the increase of texture classes, average retrieval maintains a slight fluctuation at the range of 10 percent, when the number of textures is increased from 5 to 30 classes, it is not descended quickly. So the proposed texture discrimination measure algorithms are effective for multi-kinds textures.

Experiments for distance measure criterions

In this subsection, we compare two distance measure criterions for the scaled image dataset. Retrieval algorithms use log-polar and NSCT, and NSCT employs Maxflat pyramidal decomposition and dmaxflat7 direction filter bank, the direction parameters are (Liu *et al.*, 2007; Randen and Husoy, 1999). Among every one of the six sub-groups two distance measure criterions χ^2-distance and KL divergence are adopted to get corresponding average retrieval rate, which is shown as Figure 12.

The solid line represents retrieval rate on χ^2-distance and the dashed line is the results on KL divergence. From the chart both of the two formulas own similar retrieval effectiveness. So we can get the conclusion that the retrieval effectiveness is not depended on the distance measure criterions, as the compute load of χ^2-distance is lower than KL divergence, χ^2-distance owns higher retrieval effective.

Comparison performance and parameters evaluation

In order to compare the effect of different scales and direction parameters as well as different distance measure criterions on retrieval result, this experiment uses radon transform to reduce the rotation effect and NSCT is used to decompose rotated texture image into multi-scale and multi-direction bands. Radon transform employs the nearest sampling; NSCT employs Maxflat pyramidal decomposition and

Downloaded by Wuhan University At 02:47 15 January 2019 (PT)

Sensor Review
Volume 31 · Number 2 · 2011 · 144–153

Figure 9 Texture database

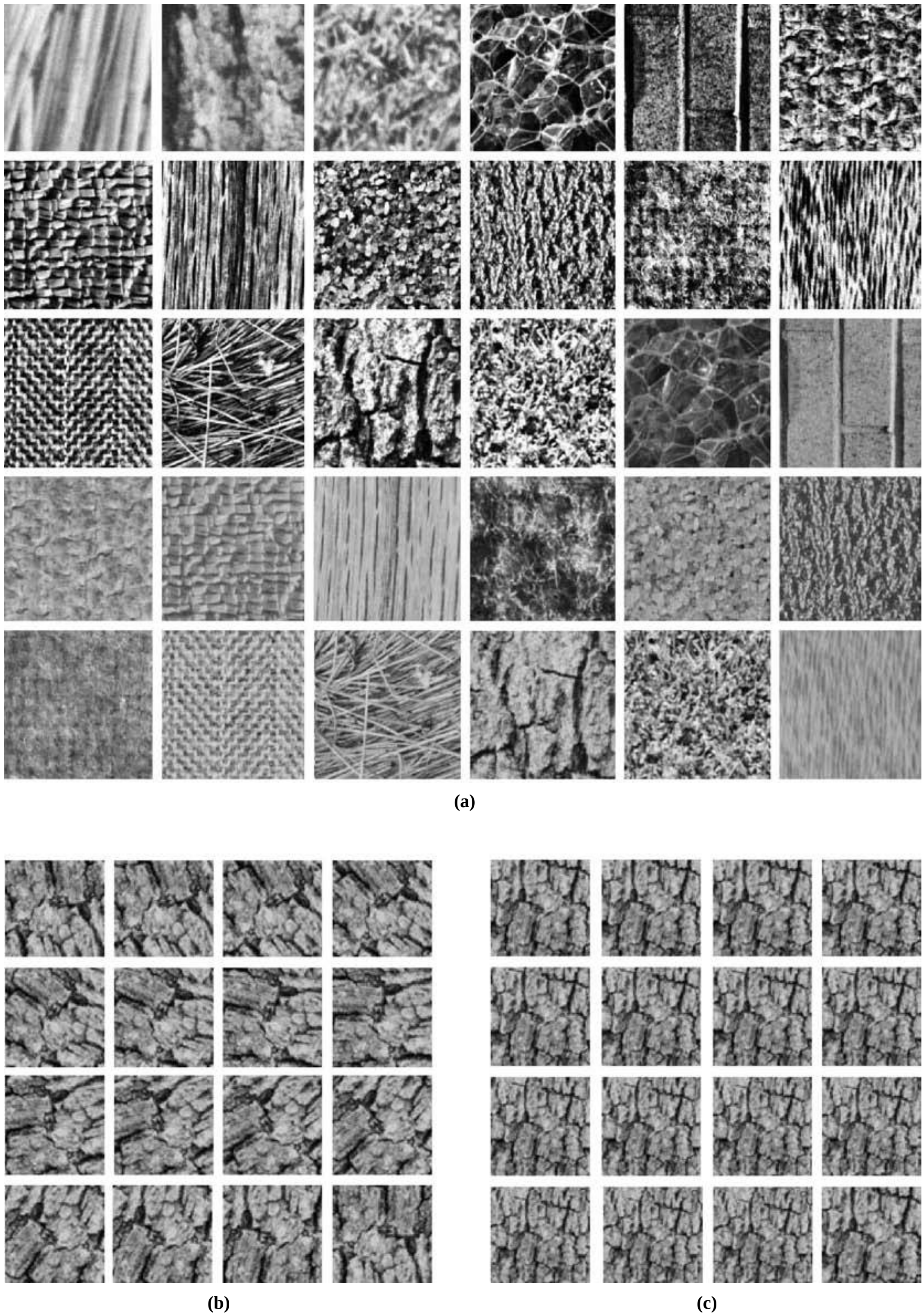

Notes: (a) 30 original texture images from VisTex dataset; (b) 16 rotated similar textures; (c) 16 scaled similar texture

dmaxflat7 direction filter bank. The selection principle of distance measure criterions is higher precision with smaller computation cost. Table II shows retrieval performances corresponding to different decomposition parameters and distance measure criterions. The dataset using joint rotation and scale set.

According to Table II, we can get the following three conclusions:

Downloaded by Wuhan University At 02:47 15 January 2019 (PT)

Figure 10 Average rates on six sub-databases on rotated-set

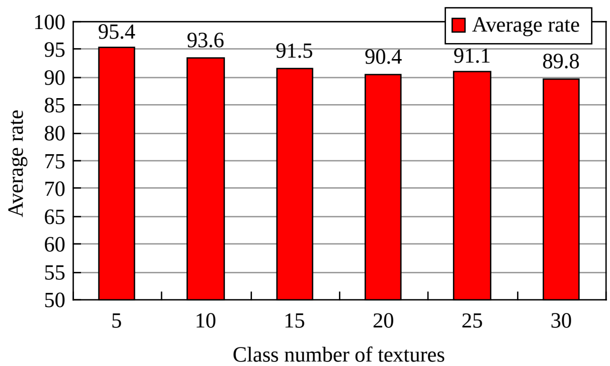

Figure 11 Average rates on six sub-databases on scaled-set

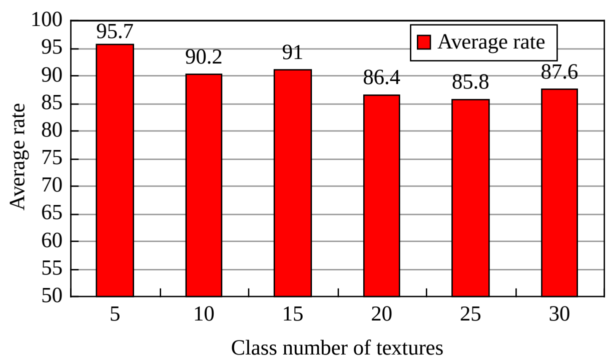

Figure 12 Comparison for two distance measure criterions: χ^2 distance and KL divergence

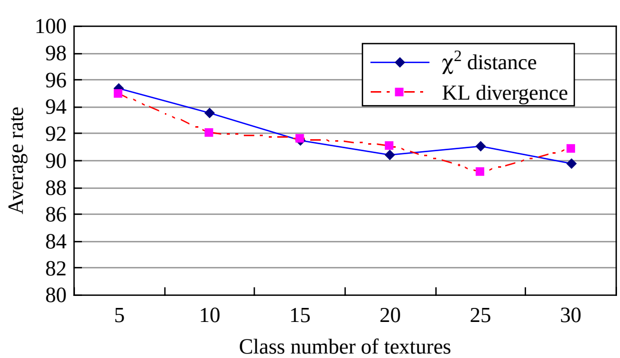

1. Whether wavelet or NSCT decomposition method, in different decomposition scales, retrieval performance will increase in the overall as the decomposition scale parameters and direction parameters increase, and the increase of scale parameters impact more evidently than the increase of direction parameters. This is consistent with the experimental one's conclusion.
2. Log-polar transform has better ability to disclination reduction than radon transform. It can also improve the retrieval performance dramatically because radon uses line integral calculating method that can provide anti-noise characteristic, but in the aspect of preserving image details it is not as good as the log-polar spectrum which is sampled from original pixels after coordinate transformation directly. The distance variable from statistical methods used in this article overlooked the spectrum disorder brought by log-polar transform, thus the retrieval efficiency is higher.
3. NSCT multi-directional multi-scale decomposition method is superior to wavelet decomposition, and the more direction and scale we use the better ability to characteristic of the image information we get.

Figure 13 is the retrieval results of two rotation-invariant texture images, where disclination reduction uses log-polar transform and multi-scale texture analysis method employs NSCT transform. D3 and D49 are used as the query image, their precision and recall ratio are, respectively, 81.3 percent and 56.3 percent. From the point of human visual effect, returned images are similar in visual effect which is consistent with human visual characteristic.

Conclusion

In this paper, we propose a novel two-level gradual rotation and scale-invariant texture retrieval algorithm, The rotation invariant relies on first feature extraction stage log-polar transform or radon transform, experiments shows that log-polar outperforms than radon in reducing the effects of rotation or scale variations of similar images on the resulting image feature. Three group experiments based on VisTex standard texture database have been done to test the algorithm's effectiveness for scaled and rotated dataset, experimental results show that the proposed feature can achieve high retrieval accuracy and outperforms the traditional wavelet packet signature image feature. Therefore, the proposed rotation and scale-invariant feature can be exploited for content-based image retrieval applications. NSCT coefficients bring us much more directional band info, but also more computational cost. Our further research focuses on the more efficient description means of large amount NSCT coefficients and the extention our algorithm to other more complicated image fields such as satellite images.

Table II Average retrieval rate of rotation-invariant retrieval based on χ^2-distance

Parameters		Average precision ratio (%)		
Rotation-reducing	**Multi-scale**	**2-12/1**	**2-24/2**	**3-20/3**
Radon	NSCT	72.4	75.8	80.6
Log-polar	NSCT	85.4	90.8	92.7
Radon	Wavelet	56.7	58.3	58.5
Log-polar	Wavelet	78.1	80.3	83.5

Downloaded by Wuhan University At 02:47 15 January 2019 (PT)

Downloaded by Wuhan University At 02:47 15 January 2019 (PT)

Figure 13 Results of rotation-invariant texture images retrieval

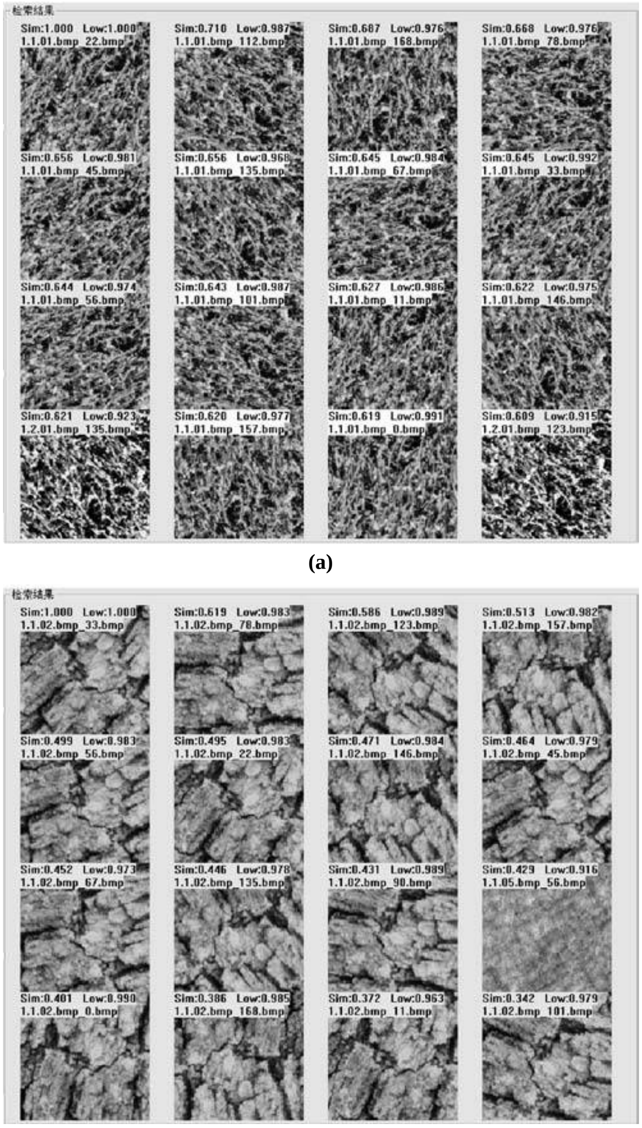

(b)

Note: (a), (b) are the retrieval results of 1.1.01 and 1.1.07 textures which are ranked by x^2-distance

References

Arivazhagan, S., Ganesan, L. and Priyal, S.P. (2006), "Texture classification using Gabor wavelets based rotation invariant features", *Pattern Recognition Letters*, Vol. 27 No. 16, pp. 1976-82.

Chen, Y.W. and Chen, Y.Q. (2008), "Invariant description and retrieval of planar shapes using radon composite features", *IEEE Transactions on Signal Processing*, Vol. 56 No. 10, pp. 4762-71.

Cheng, Q., Yang, C. and Shao, Z. (2005), "Progressive texture image retrieval based on M-band wavelet features", *Editorial Board, Geomatics and Information Science of Wuhan University*, Vol. 30 No. 5, pp. 421-524.

Chi-Man, P. (2003), "Rotation and scale invariant wavelet feature for content-based texture image retrieval", *Journal of the American Society for Information Science and Technology*, Vol. 54 No. 1, pp. 68-80.

Do, M.N. and Vetterli, M. (2002), "Wavelet-based texture retrieval using generalized Gaussian density and Kullback-Leibler distance", *IEEE Transactions on Image Processing*, Vol. 11 No. 2, pp. 146-58.

Franci, L. and Stanislav, K. (2003), "Rotation-invariant texture classification", *Pattern Recognition Letters*, Vol. 24 Nos 9-10, pp. 1151-61.

Haley, G.M. and Manjunath, B.S. (1999), "Rotation-invariant texture classification using a complete space-frequency model", *IEEE Transactions on Image Processing*, Vol. 8 No. 2, pp. 255-69.

Jafari-Khouzani, K. and Soltanian-Zadeh, H. (2005), "Rotation-invariant multi-resolution texture analysis using radon and wavelet transforms", *IEEE Transactions on Image Processing*, Vol. 14 No. 6.

Li, J.-H., Pan, Q., Chen, Y.-C., Zhang, H.-C. and Cui, P.-L. (2005), "An invariant multiscale texture image analysis algorithm based on radon transform", *Journal of Image and Graphics*, Vol. 10, No. 9.

Lin, L. and Zhang, Y. (2008), *Contourlet Transform-image Process and Application*, The Science Press, Beijing.

Liu, X. and Wang, D. (2003), "Texture classification using spectral histograms", *IEEE Transactions on Image Processing*, Vol. 12, pp. 661-70.

Liu, Y., Zhang, D., Lu, G. and Ma, W.-Y. (2007), "A survey of content-based image retrieval with high-level semantics", *Pattern Recognition*, Vol. 40 No. 1, pp. 262-82.

Lo, E.H.S., Pickering, M., Frater, M. and Amold, J. (2004), "Scale and rotation invariant texture features from the dual-tree complex wavelet transform", *Proceedings of the 2004 International Conference on Image Processing (ICIP), Singapore*, pp. 227-30.

Manjunath, B.S. and Ma, W.Y. (1996), "Texture features for browsing and retrieval of image data", *IEEE Transactions on Pattern Analysis and Machine Intelligence*, Vol. 18 No. 8, pp. 837-42.

Montoya-Zegarra, J.A., Leite, N.J. and da Silva Torres, R. (2007), "Rotation-invariant and scale-invariant steerable pyramid decomposition for texture image retrieval", *Proceedings of the 20th Brazilian Symposium on Computer Graphics and Image Processing (SIBGRAPI '07), Brazil*, pp. 121-8.

Montoya-Zegarra, J.A., Papa, J.P., Leite, N.J., Falcão, A.X. and da Silva Torres, R. (2008), "Learning how to extract rotation-invariant and scale-invariant features from texture images", *EURASIP Journal on Advances in Signal Processing*, Vol. 2008, p. P15.

Pietikäinen, M., Ojala, T. and Xu, Z. (2000), "Rotation-invariant texture classification using feature distributions", *Pattern Recognition*, Vol. 33 No. 1, pp. 43-52.

Portilla, J. and Simoncelli, E.P. (2000), "Parametric texture model based on joint statistics of complex wavelet coefficients", *International Journal of Computer Vision*, Vol. 40 No. 1, pp. 49-70.

Randen, T. and Husoy, J.H. (1999), "Filtering for texture classification: a comparative study", *IEEE Trans. Pattern Recognition Machine Intell.*, Vol. 21 No. 4, pp. 291-310.

Shao, Z., Zhu, X. and Zhang, S. (2010), "Texture retrieval for multi-source remote sensing image based on contourlet transform and spectral histogram", *Geomatics and*

Information Science of Wuhan University, Vol. 35 No. 6, pp. 723-6.

Smeulders, A.W.M., Worring, M., Santini, S., Gupta, A. and Jain, R. (2000), "Content-based image retrieval at the end of the early years", *IEEE Transactions on Pattern Analysis and Machine Intelligence*, Vol. 22 No. 12, pp. 1349-80.

Van de Wouwer, G., Scheunders, P. and Van Dyck, D. (1999), "Statistical texture characterization from discrete wavelet representations", *IEEE Transactions on Image Processing*, Vol. 8 No. 4.

Zeng, Z., Li, F., Fu, K. and Ding, C. (2005), "A method for extracting texture characters from large-scale remote sensing image", *Geomatics and Information Science of Wuhan University*, Vol. 30 No. 12, pp. 1080-3.

Zhang, D., Wong, A., Indrawan, M. and Lu, G. (2000), "Content based image retrieval using Gabor texture features", *Proceedings of the 1st IEEE Pacific-Rim Conference on Multimedia (PCM '00), 392–395, Sydney, Australia, December*.

Corresponding author

Zhenfeng Shao can be contacted at: shaozhenfeng@163.com

To purchase reprints of this article please e-mail: **reprints@emeraldinsight.com**
Or visit our web site for further details: **www.emeraldinsight.com/reprints**

Downloaded by Wuhan University At 02:47 15 January 2019 (PT)

This article has been cited by:

1. Weixun Zhou, Shawn Newsam, Congmin Li, Zhenfeng Shao. 2018. PatternNet: A benchmark dataset for performance evaluation of remote sensing image retrieval. *ISPRS Journal of Photogrammetry and Remote Sensing* **145**, 197-209. [Crossref]
2. Qimin Cheng, Zhenfeng Shao, Kang Shao, Chengyuan Li, Jinling Li, Sen Li. A distributed system architecture for high-resolution remote sensing image retrieval by combining deep and traditional features 45. [Crossref]
3. Weixun Zhou, Shawn Newsam, Congmin Li, Zhenfeng Shao. 2017. Learning Low Dimensional Convolutional Neural Networks for High-Resolution Remote Sensing Image Retrieval. *Remote Sensing* **9**:5, 489. [Crossref]
4. Konstantinos Konstantinidis, Ioannis Andreadis, Georgios Ch. Sirakoulis. Application of Artificial Intelligence Methods to Content-Based Image Retrieval 99-145. [Crossref]

Downloaded by Wuhan University At 02:47 15 January 2019 (PT)